



Published in final edited form as:

*Mol Pharm.* 2017 November 06; 14(11): 3848–3858. doi:10.1021/acs.molpharmaceut.7b00572.

## Regulation of Reduced Folate Carrier (RFC) by Vitamin D Receptor at the Blood-Brain Barrier

Camille Alam, Md.<sup>†</sup>, Tozammel Hoque<sup>†</sup>, Richard H. Finnell<sup>‡</sup>, I. David Goldman<sup>§</sup>, Reina Bendayan<sup>\*,†</sup>

<sup>†</sup>Department of Pharmaceutical Sciences, Leslie Dan Faculty of Pharmacy, University of Toronto, Toronto, Ontario M5S 3M2, Canada

<sup>‡</sup>Departments of Molecular and Cellular Biology and Medicine, Baylor College of Medicine, Houston, Texas 77030, United States

<sup>§</sup>Department of Molecular Pharmacology, Albert Einstein College of Medicine, Bronx, New York 10461, United States

### Abstract

Folates are essential for brain development and function. Folate transport in mammalian tissues is mediated by three major folate transport systems, i.e., reduced folate carrier (RFC), proton-coupled folate transporter (PCFT), and folate receptor alpha (FR $\alpha$ ), known to be regulated by ligand-activated nuclear receptors, such as vitamin D receptor (VDR). Folate uptake at the choroid plexus, which requires the actions of both FR $\alpha$  and PCFT, is critical to cerebral folate delivery. Inactivating FR $\alpha$  or PCFT mutations cause severe cerebral folate deficiency resulting in early childhood neurodegeneration. The objective of this study was to investigate the role of RFC in folate uptake at the level of the blood-brain barrier (BBB) and its potential regulation by VDR. We detected robust expression of RFC in different *in vitro* BBB model systems, particularly in immortalized cultures of human cerebral microvascular endothelial cells (hCMEC/D3) and isolated mouse brain capillaries. [<sup>3</sup>H]-methotrexate uptake by hCMEC/D3 cells at pH 7.4 was inhibited by PT523 and pemetrexed, antifolates with high affinity for RFC. We also showed that activation of VDR through calcitriol (1,25-dihydroxyvitamin D<sub>3</sub>) exposure up-regulates RFC mRNA and protein expression as well as function in hCMEC/D3 cells and isolated mouse brain capillaries. We further demonstrated that RFC expression could be down-regulated by VDR-targeting siRNA, further confirming the role of VDR in the direct regulation of this folate transporter. Together, these data suggest that augmenting RFC functional expression could constitute a novel strategy for enhancing brain folate delivery for the treatment of neurometabolic disorders caused by loss of FR $\alpha$  or PCFT function.

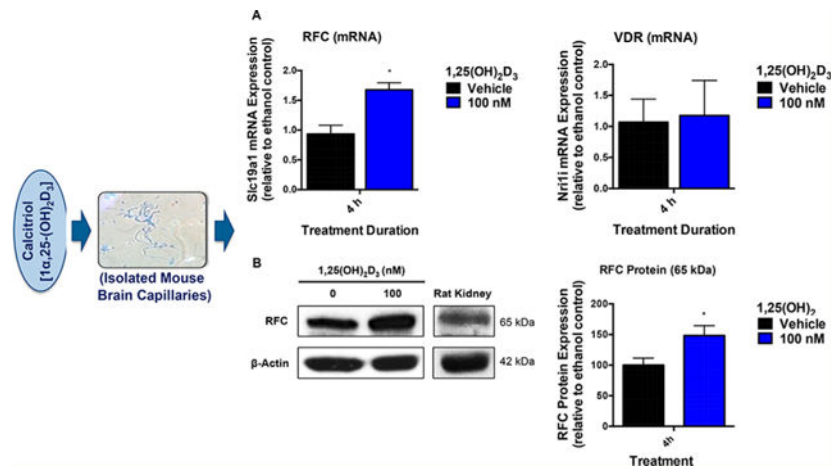
### Graphical Abstract

<sup>\*</sup>Corresponding Author: Phone: 416-978-6979; Fax: 416-978-8511; r.bendayan@utoronto.ca.

Author Contributions

C.A. and R.B. participated in research design; C.A. and M.T.H. conducted experiments; R.B. and I.D.G. contributed reagents or analytical tools; R.H.F. provided the animals; C.A., I.D.G., and R.B. performed data analysis; C.A., I.D.G., and R.B. wrote or contributed to the writing of the manuscript. All authors have given approval to the final version of the manuscript.

The authors declare no competing financial interest.



## Keywords

brain folate transport; blood-brain barrier; reduced folate carrier; vitamin D receptor

## INTRODUCTION

Folates (vitamin B9) are water-soluble vitamins that serve as one-carbon donors in nucleotide synthesis, regulation of gene expression, and production of amino acids and neurotransmitters.<sup>1</sup> Folate requirements in mammals are predominantly met through dietary sources since they lack the enzymatic capacity for folate biosynthesis. Historically, nutritional folate deficiency is one of the most common vitamin deficiencies worldwide, and continues to be so in countries that have not mandated folic acid fortification of their food supply.<sup>2</sup> Folate deficiency is associated with a variety of negative health consequences including megaloblastic anemia, failure of neural tube closure, and congenital malformations in developing embryos, as well as developmental and neurological defects in infants.<sup>3</sup> It has also been proposed to be a risk factor for cancer, heart disease, and stroke.<sup>4</sup> Maintaining sufficient folate levels requires adequate dietary intake as well as effective gastrointestinal absorption and distribution of folates to systemic tissues by specific transport systems.

Folate transport in mammalian tissues is mediated by three major transport systems: (i) the folate receptor alpha (*FR $\alpha$* ; *FOLR1*), a glycosylphosphatidylinositol-anchored receptor that binds folates with high affinity ( $K_m = 1\text{--}10\text{ nM}$ ) at pH 7.4 and facilitates transport through receptor-mediated endocytosis,<sup>5,6</sup> (ii) the proton-coupled folate transporter (PCFT; *SLC46A1*), which exhibits a relatively lower affinity for folates ( $K_m = 1\text{ }\mu\text{M}$ ) compared to *FR $\alpha$*  and functions as a proton cotransporter with optimal activity at pH 5.5,<sup>7,8</sup> and (iii) the reduced folate carrier (RFC; *SLC19A1*), with a comparable influx  $K_m$  of 2–7  $\mu\text{M}$  for reduced folate uptake at physiological pH by operating as an antiporter exchanging folates with intracellular organic phosphates.<sup>8,9</sup> Functional expression of the three folate transport systems has been reported to be modulated by nuclear receptors. These receptors belong to a large superfamily of DNA-binding transcriptional factors that regulate tissue expression of target genes in response to specific ligand activators.<sup>10</sup> The vitamin D receptor (VDR), in particular, was shown to regulate PCFT expression and function.<sup>11</sup> Treatment with the

natural VDR activating ligand, 1,25-dihydroxyvitamin D<sub>3</sub> (1,25(OH)<sub>2</sub>D<sub>3</sub>) or calcitriol, showed significant induction of *SLC46A1/Slc46a1* (PCFT) mRNA in intestinal Caco-2 cells and rat duodenal biopsies, thereby resulting in enhanced uptake of folic acid.<sup>11</sup> In the same study, the effect of VDR activation on *SLC19A1/Slc19a1* (RFC) gene expression was variable and warranted further investigation. Several other nuclear receptors, notably the estrogen receptor,<sup>12</sup> glucocorticoid receptor (GR),<sup>13</sup> hepatocyte nuclear factor 4 alpha (HNF4 $\alpha$ ),<sup>14</sup> and nuclear respiratory factor-1 (NRF-1),<sup>15</sup> are also thought to regulate mRNA and/or protein expression of major folate transporters, but their physiological roles have yet to be determined.

Folate transport in the brain is critical for the maintenance of central nervous system (CNS) homeostasis. FR $\alpha$  constitutes a major transcytosis pathway for folates across the choroid plexus epithelium.<sup>16</sup> Folate delivery into the brain occurs through the release of FR $\alpha$ -containing exosomes into the cerebrospinal fluid (CSF), which then cross the ependymal layer of the ventricles and reach the brain parenchyma through passive diffusion. PCFT has been proposed to contribute to this FR $\alpha$ -mediated transport by facilitating folate export from FR $\alpha$ -containing exosomes into the CSF, as well as from acidified endosomes within choroid plexus epithelial cells.<sup>16,17</sup> Inactivation of FR $\alpha$  or PCFT through loss-of-function mutations can impair folate uptake at the choroid plexus resulting in extremely low CSF folate levels causing the early childhood neurodegeneration disorders, cerebral folate deficiency (CFD),<sup>18,19</sup> and hereditary folate malabsorption (HFM),<sup>7,20</sup> respectively. These disorders differ in their time of onset and presentation. HFM presents within a few months after birth with failure to thrive and anemia, followed by neurological defects characterized by developmental delays, abnormal brain myelination, psychomotor regression, ataxia, and recurrent seizures. CFD, on the other hand, presents with neurological signs, alone, several years after birth since intestinal absorption and blood levels of folate are normal in this disorder. Improvement of CSF folate levels by administration of parenteral folinic acid in HFM or oral dosing in CFD improves these neurological deficits.<sup>20,21</sup>

Apart from the choroid plexus, the cerebral vascular endothelium or blood-brain barrier (BBB) represents a major route of folate delivery into the brain. Despite limited knowledge of the mechanisms of folate uptake at this site, high rates of folate delivery to the brain parenchyma appear to be consistent with the function of the vascular BBB.<sup>22–24</sup> Earlier studies conducted by Wu and Pardridge reported that transport of the major circulating form of folates, 5-methyltetrahydrofolate (5-methylTHF), into isolated human brain capillaries was saturable and sensitive to inhibition by low levels of 5-methylTHF or folic acid.<sup>23</sup> Similarly, Araújo et al. observed a saturable, time-dependent uptake of folic acid and 5-methylTHF by immortalized cultures of rat brain microvessel endothelial (RBE4) cells representative of the BBB.<sup>24</sup> Interestingly, there is also evidence suggesting the presence of RFC and PCFT at the human<sup>24</sup> and rodent BBB,<sup>25,26</sup> although their contribution to the overall brain uptake of folates has yet to be elucidated.

To date, the mechanisms of folate transport in the brain have been primarily characterized at the choroid plexus through the roles of FR $\alpha$  and PCFT. However, little is known about the functional expression of folate transporters, such as RFC and PCFT, and their regulation in brain microvessel endothelial cells which constitute the BBB. The aim of the present study

was to characterize RFC-mediated folate uptake using *in vitro* and *ex vivo* models of the BBB, as well as its potential regulation by the VDR nuclear receptor. Modulating folate uptake at the BBB through RFC could potentially represent a novel strategy for enhancing brain folate delivery for the treatment of neurometabolic disorders due to a failure of transport of folate across the choroid plexus into the CSF.

## MATERIALS AND METHODS

### Materials.

All cell culture reagents were obtained from Invitrogen (Carlsbad, CA, USA), unless indicated otherwise. Real-time quantitative polymerase chain reaction (qPCR) reagents, such as reverse transcription cDNA kits and qPCR primers, were purchased from Applied Biosystems (Foster City, CA, USA) and Life Technologies (Carlsbad, CA, USA), respectively. Primary rabbit polyclonal anti-SLC19A1 (RFC; AV44167) and anti-SLC46A1 (PCFT; SAB2108339) antibodies were obtained from Sigma-Aldrich (Oakville, ON, Canada). Mouse monoclonal anti-beta actin (sc-47778) and anti-VDR (sc-13133) antibodies were supplied by Santa Cruz Biotechnology (Dallas, TX, USA). Antirabbit or antimouse horseradish peroxidase-conjugated secondary antibodies and calcitriol (1,25(OH)<sub>2</sub>D<sub>3</sub>) were purchased from Cedarlane Laboratories (Burlington, ON, Canada). Predesigned and validated small interfering RNA (siRNA) against VDR and scrambled nonsilencing control siRNA were purchased from Santa Cruz Biotechnology (Dallas, TX, USA). Tritium-labeled [<sup>3</sup>H]-methotrexate (23.4 Ci/mmol) was purchased from Moravék Biochemicals (Brea, CA, USA). Unlabeled methotrexate was obtained from Sigma-Aldrich (Oakville, ON, Canada). Pemetrexed and PT523 were generously provided by Dr. I. D. Goldman (Albert Einstein College of Medicine, New York, USA). All buffers and Triton X-100 were purchased from Sigma-Aldrich.

### Cell Culture.

Whole cell pellets of primary cultures of human brain-derived microvascular endothelial cells (hBMEC) were kindly provided by Dr. A. Prat (University of Montreal, QC, Canada); immortalized human cerebral microvessel endothelial cell line (hCMEC/D3) was generously provided by P.O. Couraud (Institut Cochin, Département Biologie Cellulaire and INSERM, Paris, France); rat brain microvessel endothelial cell line (RBE4) was provided by Dr. F. Roux (Hôpital Fernand Widal, Paris, France). hCMEC/D3 cells (passage 27–39) were cultured in Endothelial Cell Basal Medium-2 (Lonza, Walkersville, MD, USA), supplemented with vascular endothelial growth factor, insulin-like growth factor 1, epidermal growth factor, fibroblast growth factors, hydrocortisone, ascorbate, GA-1000, heparin, and 2.5% fetal bovine serum (FBS), and grown on rat tail collagen type I-coated flasks and plates. RBE4 cells (passage 40–55) were cultured in a 50:50 mixture of minimal essential medium-alpha and HAM-F10 media supplemented with 1% penicillin/streptomycin and 10% FBS (US origin), and grown on rat tail collagen type I-coated flasks. All cell lines were maintained in a humidified incubator at 37 °C, 5% CO<sub>2</sub>, and 95% air atmosphere with fresh medium replaced every 2 to 3 days. Cells were subcultured with 0.25% trypsin-EDTA upon reaching 95% confluence. For functional studies, cells were seeded into rat tail collagen-coated 24-well plates at a density of  $6.3 \times 10^4$  cells/cm<sup>2</sup> and

subsequently used for experiments upon reaching 100% confluence (5 days). Cells used for calcitriol treatment were seeded into rat tail collagen-coated 6-well plates at an initial density of  $3.3 \times 10^4$  cells/cm<sup>2</sup> and grown to confluence for 5 days. For siRNA transfection studies, cells were plated in rat tail collagen-coated 6-well plates at an initial density of  $7.8 \times 10^4$  cells/cm<sup>2</sup> and grown to 80% confluence for 1 day before being subjected to transfection. The culture medium of plated cells was replaced every 2 days, and 24 h before the experiment.

### Rodent Brain Capillary Isolation.

Brain capillaries were isolated from adult male Wistar rats (250–300 g) and male or female C57BL/129/LM/Bc (10–12 weeks old) mice kindly provided by Dr. R. Finnell, as described previously.<sup>27</sup> Briefly, animals were anesthetized through isoflurane inhalation and decapitated once a deep anesthetic surgical plane was achieved. Brains were removed immediately and cortical gray matter was isolated and homogenized in ice-cold isolation buffer (phosphate-buffered saline or PBS containing calcium, magnesium, and supplemented with 5 mM glucose and 1 mM sodium pyruvate). Ficoll solution (30% final concentration) was added to the brain homogenates and the mixture was centrifuged at 5800 *g* for 20 min at 4 °C. The resulting pellet of capillaries was resuspended in isolation buffer supplemented with 1% bovine serum albumin (BSA) and filtered through a 300  $\mu$ m nylon mesh. The filtrate containing the capillaries was passed through a 30  $\mu$ m pluriStrainer and washed with 50 mL isolation buffer containing 1% BSA. Capillaries were harvested with 50 mL ice-cold isolation buffer and centrifuged at 1600 *g* for 5 min. The resulting pellet containing the capillaries was snap frozen in liquid nitrogen until further analysis.

### Gene Expression Analysis.

mRNA expression of specific genes of interest was quantified using qPCR. Total RNA was isolated from cell samples (hBMEC, hCMEC/D3, RBE4) and isolated rodent brain capillaries using TRIzol reagent (Invitrogen) and treated with DNase I to remove contaminating genomic DNA. RNA concentration (absorbance at 260 nm) and purity (absorbance ratio 260/280) was assessed using a Beckman Coulter DU Series 700 Scanning UV/vis Spectrophotometer. The RNA (2  $\mu$ g) was then reverse transcribed to cDNA using a high-capacity reverse transcription cDNA kit (Applied Biosystems) according to the manufacturer's instructions. Specific human/rat/mouse primer pairs for *SLC19A1/Slc19a1* (RFC; Hs00953344\_m1, Rn00446220\_m1, Mm00446220\_m1), *SLC46A1/Slc46a1* (PCFT; Hs00560565\_m1, Rn01471182\_m1, Mm00546630\_m1), *FOLR1/Folr1* (FR $\alpha$ ; Hs01124179\_91, Rn00591759\_m1, Mm00433355\_m1), and *NR1H3/Nr1h3* (VDR; Hs01045843\_m1, Mm00437297\_m1) were designed and validated by Life Technologies for use with TaqMan qPCR chemistry. All assays were done in triplicates with the housekeeping gene for human/rat/mouse cyclophilin B (Hs00168719\_m1, Rn03302274\_m1, Mm00478295\_m1) as internal control. For each gene of interest, the critical threshold cycle ( $C_T$ ) was normalized to cyclophilin B using the comparative  $C_T$  method. The difference in  $C_T$  values ( $\Delta C_T$ ) between the target gene and cyclophilin B was then normalized to the corresponding  $C_T$  of the vehicle control ( $C_{T, VC}$ ) and expressed as fold expression ( $2^{-\Delta\Delta C_T}$ ) to assess the relative difference in mRNA expression for each gene.

### Protein Expression Analysis.

Western blotting was performed according to our published protocol with minor modifications.<sup>28</sup> Briefly, whole cell or brain capillary lysates were obtained after lysing cells and rodent brain capillaries with a modified RIPA buffer [50 mM Tris pH 7.5, 150 mM NaCl, 1 mM EGTA, 1 mM sodium *o*-vanadate, 0.25% (v/v) sodium deoxycholic acid, 0.1% (v/v) sodium dodecyl sulfate (SDS), 1% (v/v) NP-40, 200  $\mu$ M PMSF, 0.1% (v/v) protease inhibitor]. Protein concentration of the lysates was quantified using Bradford's protein assay (Bio-Rad Laboratories) with BSA as the standard. For each sample, total protein (50  $\mu$ g) was mixed in Laemmli buffer and 10%  $\beta$ -mercaptoethanol, separated on 10% SDS-polyacrylamide gel, and electrotransferred onto a polyvinylidene fluoride membrane overnight. The blots were blocked for 2 h at room temperature in 5% skim milk Tris-buffered saline solution containing 0.1% Tween 20 and incubated overnight at 4 °C with primary rabbit polyclonal anti-SLC19A1 (RFC) antibody (1:250), rabbit polyclonal anti-SLC46A1 (PCFT) antibody (1:250), murine monoclonal anti-VDR antibody (1:250), and murine monoclonal anti-beta actin antibody (1:1000). The blots were incubated for 1.5 h with corresponding horseradish peroxidase-conjugated antirabbit (1:5000) or antimouse (1:5000) secondary antibody. Protein bands were detected using enhanced chemiluminescence Super-Signal West Pico System (Thermo Fisher Scientific) and autoradiographed onto X-ray film.

### Transport Assays.

Functional assays with tritium-labeled [<sup>3</sup>H]-methotrexate were performed following standard procedures from our laboratory with minor modifications.<sup>29</sup> All experiments were performed using transport buffer consisting of Hanks' balanced salt solution (HBSS) supplemented with 0.01% BSA and 25 mM HEPES (pH 7.4). Confluent hCMEC/D3 cell monolayers grown on 24-well plates were washed twice with transport buffer (pH 7.4) and then preincubated in the same buffer at 37 °C for 20 min. Transport was initiated by adding 0.5 mL of transport buffer (pH 7.4) containing 50 nM [<sup>3</sup>H]-methotrexate at 37 °C. To examine the inhibitory effects of folate analogs with high affinity for RFC, these agents were added to both preincubation and radioactive transport buffers. At the desired interval, the radioactive medium was aspirated and cells were washed twice with ice-cold PBS and solubilized in 1 mL of 1% Triton X-100 at 37 °C for 40 min. The content of each well was collected and mixed with 3 mL of PicoFluor 40 scintillation fluid (PerkinElmer Life and Analytical Sciences), and total radioactivity was measured with a Beckman Coulter LS6500 Scintillation counter. For each experiment, correction for nonspecific binding and variable quench time was conducted by estimating the retention of radiolabeled compound in the cells after a minimum (zero) time of exposure. The "zero time" uptake (background) was determined by removing the radiolabeled solution immediately after its introduction into the well, followed by two washes of ice-cold PBS and collection of cells for liquid scintillation counting. Cellular uptake of the radiolabeled methotrexate was normalized to total protein content per well, which was measured by using the Bio-Rad DC Protein Assay kit with BSA as the standard.



### Calcitriol Treatment.

Confluent hCMEC/D3 cell monolayers grown on 6-well plates were treated with either ethanol (vehicle control) or calcitriol (50–500 nM) for a period of 6 or 24 h at 37 °C. Freshly isolated mouse brain capillaries resuspended in 200  $\mu$ L isolation buffer were also exposed to ethanol (vehicle control) or 100 nM calcitriol for 4 h at room temperature. At the desired time interval, treated cells or brain capillaries were harvested using TRIzol or RIPA lysis buffer and subsequently processed for gene and protein analyses, respectively. The effect of calcitriol on methotrexate uptake was further examined by treating hCMEC/D3 cell monolayers with 500 nM calcitriol for 24 h before conducting transport assays with [<sup>3</sup>H]-methotrexate at pH 7.4 and 37 °C. To ensure that cells remained viable during treatment, all concentrations of calcitriol used in this study were tested with tetrazolium salts (MTT) assay. We confirmed that there was no significant reduction in cell viability in the calcitriol-treated groups compared to vehicle-treated or untreated controls (data not shown). The dose-dependent effect of calcitriol on *SLC19A1* (RFC) mRNA expression was also assessed by exposing hCMEC/D3 cells to a wide range of calcitriol concentrations (0.1–500 nM) for 24 h. In all of the tested concentrations, RFC mRNA was induced by 40–50% relative to vehicle (data not shown).

### siRNA Treatment.

hCMEC/D3 cells plated in 6-well plates were subjected to siRNA transfection upon reaching 80% confluence (24 h). The transfection mix was prepared in Opti-MEM (Invitrogen) medium containing control or VDR siRNA and Lipofectamine RNAi MAX (Invitrogen) according to the manufacturer's protocol. The final concentration of siRNA and Lipofectamine added to the cells were 100 nM and 2  $\mu$ L/ml, respectively. Cells were cultured in the presence of transfection mixture for 24 h before replacing with fresh hCMEC/D3 cell medium the following day. Cells were grown for an additional 48 h before being harvested and used for Western blotting analysis to determine VDR and RFC protein expression.

### Data Analysis.

All experiments were repeated at least three times using cells from different passages or different rodent brain capillary preparations. Each data point from a single experiment represents triplicate measurements. Results are presented as mean  $\pm$  SEM. All statistical analyses were performed using Prism 6 software (GraphPad Software Inc., San Diego, CA, USA). Statistical significance between two groups was assessed by two-tailed Student's *t* test for unpaired experimental values. Multiple group comparisons were performed using one-way analysis of variance (ANOVA) with Bonferroni's posthoc test.  $p < 0.05$  was considered statistically significant.

## RESULTS

### Expression of Folate Receptor/Transporters at the BBB.

Relative mRNA and protein expression of RFC, PCFT, and FR $\alpha$  were documented in various *in vitro* and *ex vivo* models representative of the BBB (i.e., immortalized human

(hCMEC/D3) and rat (RBE4) brain microvessel endothelial cell lines, primary cultures of human brain-derived microvascular endothelial cells (hBMEC), and isolated rat and mouse brain capillaries) by qPCR and Western blot analysis, respectively. Robust mRNA expression of *SLC19A1/Slc19a1* (RFC) and *SLC46A1/Slc46a1* (PCFT) was detected in all BBB model systems, particularly in the isolated rodent brain capillaries (Figure 1). Interestingly, *FOLR1/Folr1* (FR $\alpha$ ) was not detected in human brain microvessel endothelial cells but was present in rodent brain capillaries. Corresponding Western blots also revealed multiple protein bands for RFC (58–75 kDa) and PCFT (50–63 kDa) (Figure 1B). The multiple migratory protein bands could be attributed to post-translational modifications, such as differential glycosylation of N-linked glycosylation sites of these transmembrane proteins, as previously demonstrated by various groups<sup>30,31</sup> and our own laboratory through deglycosylation reactions (data not shown).

### Methotrexate Uptake by hCMEC/D3 Cells.

The functional activity of folate transporters at the BBB was examined by performing transport assays with tritium-labeled [<sup>3</sup>H]-methotrexate using the well-characterized hCMEC/D3 cell line as an *in vitro* model of the human BBB. Transport assays were performed at extracellular pH 7.4, reflecting optimal activity for RFC and the presumed neutral pH of the BBB interface due to the high arterial blood flow at this site.<sup>8</sup> Methotrexate is an established RFC substrate ( $K_m \sim 1\text{--}7 \mu\text{M}$ ) and has been used in numerous studies to assess RFC-mediated transport.<sup>8,9</sup> In hCMEC/D3 cells, uptake of [<sup>3</sup>H]-methotrexate was inhibited by PT523 (~50%) or pemetrexed (~70%), high-affinity substrates for this transporter, (i.e.,  $K_i$  of 0.2 and 1  $\mu\text{M}$ , respectively).<sup>32</sup> Influx was also inhibited by excess nonlabeled MTX (~70%) (Figure 2).

### Effect of Calcitriol Treatment on RFC Expression in hCMEC/D3 Cells.

The regulation of RFC by VDR nuclear receptor was further assessed using the hCMEC/D3 cell line. Initially, qPCR analysis was used to confirm the presence of VDR in two different systems representative of the human (hCMEC/D3 cells) and rodent (isolated mouse brain capillaries) BBB (Figure 3A). To examine the effect of VDR activation on RFC expression, hCMEC/D3 cells were exposed to increasing concentrations of the VDR ligand, 1,25(OH)<sub>2</sub>D<sub>3</sub> or calcitriol, for 6 or 24 h. *NR1H3* (VDR) mRNA expression was unchanged following calcitriol treatment (Figure 3B). *SLC19A1* (RFC) mRNA expression was induced by approximately 1.5-fold after exposure to 50–500 nM calcitriol for 6 and 24 h (Figure 3B). Similarly, RFC protein was increased by nearly 50% following 24 h treatment with 500 nM calcitriol, and this induction was consistent for the different glycosylated forms of RFC detected at 65 and 75 kDa (Figure 3C). Significant increases in PCFT mRNA and protein expression was also observed following exposure to calcitriol, which is in agreement with what was previously observed in the intestine (data not shown).<sup>11</sup> However, it should be noted that PCFT might be a less relevant folate transporter at this site due to the presumed neutral pH at the BBB and the low pH optimum of PCFT.

### Effect of Calcitriol Treatment on RFC Function in hCMEC/D3 Cells.

To verify whether the RFC induction following calcitriol exposure would also lead to an enhancement in its functional activity, transport assays were subsequently conducted in



hCMEC/D3 cells treated with calcitriol (500 nM) or ethanol (vehicle control) for 24 h. Uptake of [<sup>3</sup>H]-methotrexate between 5 s to 1 min was increased by 30–40% in calcitriol-treated cells compared to vehicle control (Figure 4A). [<sup>3</sup>H]-methotrexate uptake by induced hCMEC/D3 cells, measured after 1 min, was also effectively blocked by pemetrexed suggesting that the transport was specifically mediated by RFC (Figure 4B).

#### Down-Regulation of RFC Expression by VDR siRNA in hCMEC/D3 Cells.

VDR targeting siRNA was used to further confirm the direct involvement of VDR in the regulation of RFC in hCMEC/D3 cells. Transfection of cells with VDR siRNA resulted in more than 50% down-regulation of VDR protein expression (Figure 5). A corresponding decrease in RFC expression by 30–40% was also observed in VDR siRNA-treated cells compared to scrambled siRNA-transfected controls, as depicted by protein bands between 63 and 75 kDa. Similar reduction in PCFT protein levels were also observed in hCMEC/D3 cells transfected with VDR siRNA relative to control (data not shown).

#### Effect of Calcitriol Treatment on RFC Expression in Isolated Mouse Brain Capillaries.

The effect of calcitriol-mediated activation of VDR on RFC expression was additionally investigated in isolated mouse brain capillaries, which are considered to be a robust *ex vivo* model of the BBB. Treatment of mouse brain capillaries with 100 nM calcitriol for 4 h showed over 50% increase in *Slc19a1* mRNA and a corresponding 50% induction in RFC protein, supporting our *in vitro* findings and further demonstrating the role of VDR in regulating RFC expression (Figure 6).

## DISCUSSION

Folates play a crucial role in the development and function of the CNS. Folate uptake at the choroid plexus, which requires the actions of FR $\alpha$  and PCFT, is critical to cerebral folate delivery.<sup>16,17,20</sup> As previously indicated, folate uptake at the choroid plexus begins with FR $\alpha$ -mediated transcytosis, followed by the export of folates from FR $\alpha$ -containing exosomes directly into the CSF, presumably via PCFT.<sup>16,17</sup> PCFT-mediated folate export from acidified endosomes into the cytoplasm may also occur within choroid plexus epithelial cells. Since RFC is expressed at the apical membrane of these cells, it could also serve as a route for folate efflux into the CSF.<sup>25</sup> Inactivating FR $\alpha$  or PCFT mutations can cause severe CSF folate deficiency, affecting progenitor-rich CNS tissues situated in proximity to the cerebral ventricles, and resulting in early childhood neurological disorders, such as CFD<sup>18,19</sup> and HFM,<sup>7,20</sup> respectively. Although there is an overlap in the neurological defects associated with these two disorders, there are differences in their clinical presentation. HFM is associated with impaired intestinal folate absorption resulting in systemic folate deficiency, as well as impaired folate transport into the CSF causing neural folate deficiency. Signs and symptoms related to HFM such as anemia and immune deficiency occur within a few months of birth, while the neurological consequences usually come later.<sup>20</sup> On the other hand, patients with CFD are normal at birth and throughout infancy and only exhibit neurological deficits at 2–3 years of age.<sup>21</sup>

Apart from the choroid plexus, the vascular BBB represents an arterial route that provides folate to a substantial portion of the brain.<sup>22–24</sup> There are several reports that 5-methylTHF is transported into the brain via the BBB.<sup>23,24</sup> There is also evidence confirming the presence of folate transport systems, RFC and PCFT, at the human<sup>24</sup> and rodent BBB.<sup>25,26</sup> Substantial folate delivery at the vascular BBB is further exemplified by the fact that despite the absence of CSF folate in HFM or CFD, some patients with HFM exhibit minimal neurological defects, and the onset of CFD-related complications only occur a few years after birth. One explanation for why HFM has an earlier onset than CFD is that the extremely low blood folate levels limits the protective effect of folate delivery across the BBB.<sup>20</sup> In contrast, despite normal blood folate levels in patients with CFD and presumed normal folate uptake at the BBB, the loss of FR $\alpha$  function and consequent low CSF folate levels ultimately lead to neurological deficits, indicating that there may be insufficient folate transport across the BBB to adequately supply neural cells in proximity to the ventricles with folates that are normally supplied via the CSF.<sup>33,34</sup> Therefore, investigating the functional role of folate transport systems (i.e., RFC) at the level of the BBB and modulating folate uptake through interactions with specific nuclear receptors (i.e., VDR) could potentially increase folate uptake into the CNS, especially when the contribution of folate delivery to the CSF from the choroid plexus is impaired.

In this study, we detected mRNA expression of *SLC19A1/Slc19a1* (RFC) and *SLC46A1/Slc46a1* (PCFT) in various human and rodent BBB model systems (Figure 1A). *FOLR1/Folr1* (FR $\alpha$ ) mRNA was not detected in human brain microvessel endothelial cells (hCMEC/D3 and hBMEC) but was present in isolated rodent brain capillaries, suggesting species-specific differences in the expression of this receptor. Our gene expression data corroborates previous findings by others in that RFC and PCFT are expressed in both human<sup>24</sup> and rodent BBB.<sup>25,26</sup> Several studies have also confirmed the absence of FR $\alpha$  in an *in vitro* model of the human BBB<sup>24</sup> and in different regions of human brain tissues except for the choroid plexus.<sup>18</sup> Corresponding Western blots confirmed our qPCR results and showed multiple protein bands for RFC (58–75 kDa) and PCFT (50–63 kDa) (Figure 1B). Previously, both transporters have been detected at different molecular sizes in various cell lines and species,<sup>35,36</sup> most of which are within the range of molecular weights reported here. This variability in folate transporter migration could be attributed to the differential glycosylation of these transmembrane proteins at their respective N-linked glycosylation sites.<sup>30,31</sup> Wong et al. have shown that although human RFC only possess a single glycosylation site (Asn 58), it undergoes heavy glycosylation that could result in up to 20 kDa increase in its molecular weight.<sup>30</sup> Similarly, Unal et al. detected multiple protein bands (~35–55 kDa) for human PCFT in HeLa cells, which they confirmed to be due to variability in the glycosylation of this transporter.<sup>31</sup>

Although PCFT was detected in all of the BBB model systems, it might be a less relevant transporter at this site due to the neutral pH at the BBB interface and the low pH required for optimal PCFT uptake. Therefore, functional assays focused on the characterization of folate uptake at pH 7.4 that is most likely mediated by RFC. To investigate the contribution of RFC to folate uptake at the BBB, [<sup>3</sup>H]-methotrexate uptake was investigated using an *in vitro* model of the human BBB (hCMEC/D3 cells). The hCMEC/D3 cell line was specifically chosen for this work as it retains many of the *in vivo* morphological and biochemical

properties of the human brain microvascular endothelium, including functional expression of tight junction proteins, endothelial cell markers, and drug efflux/influx transporters.<sup>37</sup> In hCMEC/D3 cells, the specificity of [<sup>3</sup>H]-methotrexate uptake at pH 7.4 was assessed in the presence 10  $\mu$ M PT523 or pemetrexed, which are potent inhibitors of RFC with  $K_i$ 's of 0.2 and 1  $\mu$ M, respectively.<sup>32</sup> These compounds exhibited an inhibitory effect of 50–70% (Figure 2), corroborating previous studies demonstrating potent inhibition by PT523 or pemetrexed of methotrexate uptake in HepG2 cells.<sup>32</sup> Taken together, these findings demonstrate functional expression of RFC in an *in vitro* model of the human BBB, suggesting a potential role for this transporter in mediating folate uptake at this site.

Although transport properties of RFC have been extensively examined in several mammalian cells and tissues, relatively little is known about its regulatory mechanisms. A few reports in the literature suggest that RFC can be modulated by ligand-activated transcriptional factors or nuclear receptors.<sup>15,38</sup> In HeLa cells, Gonen and Assaraf have shown that NRF-1 could act as an inducible transcriptional regulator of RFC since siRNA silencing of this nuclear receptor resulted in a moderate but significant reduction in *SLC19A1* mRNA expression.<sup>15</sup> In contrast, RFC functional expression in rat liver was reported to be down-regulated by the aryl hydrocarbon receptor following exposure to its activating ligand, dioxin.<sup>38</sup> Previous work by Eloranta et al. also indicated that VDR could up-regulate the expression and functional activity of folate transporters, such as PCFT and potentially RFC, in the intestine.<sup>11</sup> At the BBB, VDR expression has been detected in human (hCMEC/D3) and rat (RBE4) brain microvessel endothelial cells as well as in isolated rat brain capillaries.<sup>39</sup> Activation of VDR by calcitriol ( $K_m$  in the pM range) has also been shown to regulate the functional expression of a wide range of membrane-associated drug transporters (i.e., P-gp, MRP2, MRP4, OATP1A2) in the brain<sup>39,40</sup> and other tissues.<sup>41</sup> In this study, the potential role of VDR in the context of RFC regulation at the BBB was examined. We confirmed that *NRIII* (VDR) mRNA is expressed in our BBB model systems (hCMEC/D3 cells and isolated mouse brain capillaries) (Figure 3A). Exposure of hCMEC/D3 cells to 50–500 nM of calcitriol resulted in nearly 50% induction of RFC mRNA and protein expression (Figure 3B,C). Transport assays with methotrexate also showed a corresponding increase in RFC functional activity (up to 40%) in hCMEC/D3 cells treated with calcitriol compared to control (Figure 4). To further verify the involvement of VDR, mRNA and protein up-regulation of PCFT, a known VDR target, was also documented (data not shown).<sup>11</sup> These results are most exciting as they demonstrate for the first time that ligand-dependent activation of VDR through calcitriol treatment can up-regulate RFC functional expression in an *in vitro* human BBB model. Moreover, transfection of hCMEC/D3 cells with VDR-targeting siRNA reduced RFC protein by approximately 40% relative to control, further demonstrating the role of VDR in modulating RFC expression (Figure 5). To confirm our *in vitro* findings, the effect of VDR activation on RFC expression was also investigated in isolated mouse brain capillaries, where treatment with calcitriol resulted in an up-regulation of RFC mRNA and protein levels (40–50%) that are comparable to what was observed in the hCMEC/D3 cell line (Figure 6). Taken together, these findings strongly suggest for the first time that VDR is directly involved in the regulation of RFC expression and function in human brain microvessel endothelial cells or mouse brain capillaries that are representative of the BBB.

Modulation of folate uptake at the BBB through RFC may have clinical importance due to the lack of established optimal therapy for childhood neurodegenerative disorders caused by mutations in *FR $\alpha$*  or PCFT. The standard approach to the treatment of CFD and HFM is to increase folate levels in the CSF through administration of oral folinic acid for the former and parenteral folinic acid for the latter.<sup>20,21</sup> Folinic acid (leucovorin or 5-formyltetrahydrofolate) is a stable form of folate, a good RFC substrate ( $K_m = 2\text{--}7\ \mu\text{M}$ ), and the preferred treatment for these disorders. Despite significant increases in systemic folate concentrations in response to folinic acid intervention, it is a challenge to achieve even near normal CSF folate levels in infants and children sufficient to correct these neurological complications.<sup>20,42,43</sup> Folate concentration in the CSF varies with age and is at its highest during infancy and early childhood at  $\sim 100\text{--}150\ \text{nM}$ , then decreasing to  $\sim 50\text{--}90\ \text{nM}$  by the age of six, and  $>60\ \text{nM}$  during puberty.<sup>44,45</sup> Thus, our present findings could lead to the development of promising approaches to enhance the delivery of folate to the brain via RFC at the BBB. However, it should also be noted that since VDR is a key regulator of numerous drug transporters (i.e., P-gp, MRP2, MRP4, OATP1A2) and drug-metabolizing enzymes (i.e., cytochrome P450s, SULT2A1),<sup>39,41,46</sup> its activation could also interfere with normal body functions including folate homeostasis. In particular, P-gp and MRPs have been documented to be low affinity ( $K_m = 0.2\text{--}2\ \text{mM}$ ) efflux transporters of folates and their functional activity could oppose folate uptake mediated by RFC.<sup>47</sup> Additionally, calcitriol-mediated activation of VDR may further affect calcium homeostasis through transactivation of calcium ion channels in the kidney and intestine (i.e., TRPV5 and TRPV6) that could lead to increased plasma calcium levels.<sup>48</sup> Taken together, calcitriol supplementation may require strict monitoring to establish a fine balance between the risks and benefits of VDR activation.

In summary, we detected RFC expression and function in different *in vitro* systems representative of the BBB, particularly in the hCMEC/D3 cell line. We also provided evidence that activation of VDR through calcitriol exposure up-regulates RFC mRNA and protein expression as well as function in hCMEC/D3 cells or isolated mouse brain capillaries. We further demonstrated that RFC expression could be down-regulated by VDR-targeting siRNA, further confirming the role of VDR in the direct regulation of this folate transporter. Together, these data suggest that augmenting RFC functional expression through activation of VDR could constitute a novel strategy for enhancing brain folate delivery for the treatment of neurometabolic disorders caused by loss of *FR $\alpha$*  or PCFT function at the level of the choroid plexus.

## ACKNOWLEDGMENTS

We thank Dr. Robert Steinfeld (University Medical Center Göttingen, Göttingen, Germany) and Dr. Bogdan Włodarczyk (Baylor College of Medicine, Texas, USA) for their insights on this work. We also thank Theodora Bruun, Marc Li, and Adrian Turner for their technical assistance. This research was supported by an operating grant from the Natural Sciences and Engineering Research Council of Canada (NSERC) awarded to Dr. Reina Bendayan. Camille Alam is a recipient of an Ontario Graduate Scholarship, Centre for Pharmaceutical Oncology Scholarship, and Pfizer Canada Graduate Fellowship. Dr. Richard Finnell was supported by NIH grants R01HD081216 and R01HD083809. Dr. I. David Goldman was supported by a National Cancer Institute grant CA082621.

## ABBREVIATIONS

<b>1,25(OH)<sub>2</sub>D<sub>3</sub></b>	1,25-dihydroxyvitamin D <sub>3</sub>
<b>BBB</b>	blood-brain barrier
<b>CFD</b>	cerebral folate deficiency
<b>CNS</b>	central nervous system
<b>CSF</b>	cerebrospinal fluid
<b>FR<math>\alpha</math></b>	folate receptor alpha
<b>hBMEC</b>	primary cultures of human brain-derived microvascular endothelial cells
<b>hCMEC/D3</b>	immortalized cultures of human cerebral microvessel endothelial cells
<b>HFM</b>	hereditary folate malabsorption
<b>PCFT</b>	proton-coupled folate transporter
<b>qPCR</b>	quantitative polymerase chain reaction
<b>RBE4</b>	immortalized cultures of rat brain microvessel endothelial cells
<b>RFC</b>	reduced folate carrier
<b>siRNA</b>	small interfering RNA
<b>VDR</b>	vitamin D receptor

## REFERENCES

- (1). Tibbetts AS; Appling DR Compartmentalization of mammalian folate-mediated one-carbon metabolism. *Annu. Rev. Nutr* 2010, 30, 57–81. [PubMed: 20645850]
- (2). Bailey RL; West KP; Black RE The epidemiology of global micronutrient deficiencies. *Ann. Nutr. Metab* 2015, 66 (2), 22–33.
- (3). Surtees R Cobalamin and folate responsive disorders Vitamin responsive conditions on pediatric neurology, International review of child neurology series; Baxter P, Ed.; Mac Keith Press: London, 2001.
- (4). Bailey LB; Rampersaud GC; Kauwell GPA Folic acid supplements and fortification affect the risk for neural tube defects, vascular disease and cancer: evolving science. *J. Nutr* 2003, 133 (6), 1961S–1968S. [PubMed: 12771346]
- (5). Kamen BA; Smith AK A review of folate receptor alpha cycling and 5-methyltetrahydrofolate accumulation with an emphasis on cell models in vitro. *Adv. Drug Delivery Rev* 2004, 56 (8), 1085–1097.
- (6). Elnakat H; Ratnam M Distribution, functionality and gene regulation of folate receptor isoforms: Implications in targeted therapy. *Adv. Drug Delivery Rev* 2004, 56 (8), 1067–1084.
- (7). Qiu A; Jansen M; Sakaris A; Min SH; Chattopadhyay S; Tsai E; Sandoval C; Zhao R; Akabas MH; Goldman ID Identification of an intestinal folate transporter and the molecular basis for hereditary folate malabsorption. *Cell* 2006, 127 (5), 917–928. [PubMed: 17129779]

- (8). Zhao R; Goldman ID Folate and thiamine transporters mediated by facilitative carriers (SLC19A1–3 and SLC46A1) and folate receptors. *Mol. Aspects Med* 2013, 34 (2–3), 373–385. [PubMed: 23506878]
- (9). Matherly LH; Hou Z Structure and function of the reduced folate carrier: a paradigm of a major facilitator superfamily mammalian nutrient transporter. *Vitam. Horm* 2008, 79, 145–184. [PubMed: 18804694]
- (10). Benoit R; Cooney A; Giguere V; Ingraham H; Lazar M; Muscat G; et al. International Union of Pharmacology. LXVI. Orphan Nuclear Receptors. *Pharmacol. Rev* 2006, 58 (4), 798–836. [PubMed: 17132856]
- (11). Eloranta JJ; Zair ZM; Hiller C; Hausler S; Stieger B; Kullak-Ublick GA Vitamin D3 and its nuclear receptor increase the expression and activity of the human proton-coupled folate transporter. *Mol. Pharmacol* 2009, 76 (5), 1062–1071. [PubMed: 19666701]
- (12). Kelley KMM; Rowan BG; Ratnam M Modulation of the folate receptor a gene by the estrogen receptor: mechanism and implications in tumor targeting. *Cancer Res* 2003, 63 (11), 2820–2828. [PubMed: 12782587]
- (13). Tran T; Shatnawi A; Zheng X; Kelley KMM; Ratnam M Enhancement of folate receptor alpha expression in tumor cells through the glucocorticoid receptor: a promising means to improved tumor detection and targeting. *Cancer Res.* 2005, 65 (10), 4431–4442. [PubMed: 15899836]
- (14). Salbaum JM; Finnell RH; Kappen C Regulation of folate receptor 1 gene expression in the visceral endoderm. *Birth Defects Res., Part A* 2009, 85 (4), 303–313.
- (15). Gonen N; Assaraf YG The obligatory intestinal folate transporter PCFT (SLC46A1) is regulated by nuclear respiratory factor 1. *J. Biol. Chem* 2010, 285 (44), 33602–33613. [PubMed: 20724482]
- (16). Grapp M; Wrede A; Schweizer M; Hüwel S; Galla H-J; Snaidero N; Simons M; Bückers J; Low PS; Urlaub H; et al. Choroid plexus transcytosis and exosome shuttling deliver folate into brain parenchyma. *Nat. Commun* 2013, 4, 2123. [PubMed: 23828504]
- (17). Zhao R; Min SH; Wang Y; Campanella E; Low PS; Goldman ID A role for the proton-coupled folate transporter (PCFT-SLC46A1) in folate receptor-mediated endocytosis. *J. Biol. Chem* 2009, 284 (7), 4267–4274. [PubMed: 19074442]
- (18). Steinfeld R; Grapp M; Kraetzner R; Dreha-Kulaczewski S; Helms G; Dechent P; Wevers R; Grosso S; Gartner J Folate receptor alpha defect causes cerebral folate transport deficiency: a treatable neurodegenerative disorder associated with disturbed myelin metabolism. *Am. J. Hum. Genet* 2009, 85 (3), 354–363. [PubMed: 19732866]
- (19). Grapp M; Just I. a.; Linnankivi T; Wolf P; Lücke T; Hausler M; Gartner J; Steinfeld R Molecular characterization of folate receptor 1 mutations delineates cerebral folate transport deficiency. *Brain* 2012, 135 (7), 2022–2031. [PubMed: 22586289]
- (20). Zhao R; Aluri S; Goldman ID The proton-coupled folate transporter (PCFT-SLC46A1) and the syndrome of systemic and cerebral folate deficiency of infancy: hereditary folate malabsorption. *Mol. Aspects Med* 2017, 53, 57–72. [PubMed: 27664775]
- (21). Hyland K; Shoffner J; Heales SJ Cerebral folate deficiency. *J. Inherited Metab. Dis* 2010, 33 (5), 563–570. [PubMed: 20668945]
- (22). Pardridge WM Drug transport across the blood–brain barrier. *J. Cereb. Blood Flow Metab* 2012, 32 (11), 1959–1972. [PubMed: 22929442]
- (23). Wu D; Pardridge WM Blood-brain barrier transport of reduced folic acid. *Pharm. Res* 1999, 16 (3), 415–419. [PubMed: 10213373]
- (24). Araújo JR; Goncalves P; Martel F Characterization of uptake of folates by rat and human blood-brain barrier endothelial cells. *BioFactors* 2010, 36 (3), 201–209. [PubMed: 20232349]
- (25). Wang Y; Zhao R; Russell RG; Goldman ID Localization of the murine reduced folate carrier as assessed by immunohistochemical analysis. *Biochim. Biophys. Acta, Biomembr* 2001, 1513 (1), 49–54.
- (26). Wang X; Cabrera RM; Li Y; Miller DS; Finnell RH Functional regulation of P-glycoprotein at the blood-brain barrier in proton-coupled folate transporter (PCFT) mutant mice. *FASEB J.* 2013, 27 (3), 1167–1175. [PubMed: 23212123]



- (27). Chan GNY; Cannon RE Assessment of ex vivo transport function in isolated rodent brain capillaries. *Curr. Protoc. Pharmacol* 2017, 76, 1–16.
- (28). Hoque MT; Shah A; More V; Miller DS; Bendayan R In vivo and ex vivo regulation of breast cancer resistant protein (Bcrp) by peroxisome proliferator-activated receptor alpha (Ppara.) at the blood-brain barrier. *J. Neurochem* 2015, 135 (6), 1113–1122. [PubMed: 26465636]
- (29). Kis O; Zastre JA; Ramaswamy M; Bendayan R pH dependence of organic anion-transporting polypeptide 2B1 in Caco-2 cells: potential role in antiretroviral drug oral bioavailability and drug-drug interactions. *J. Pharmacol. Exp. Ther* 2010, 334 (3), 1009–1022. [PubMed: 20507927]
- (30). Wong SC; Zhang L; Proefke SA; Matherly LH Effects of the loss of capacity for N-glycosylation on the transport activity and cellular localization of the human reduced folate carrier. *Biochim. Biophys. Acta, Biomembr* 1998, 1375 (1–2), 6–12.
- (31). Unal ES; Zhao R; Qiu A; Goldman ID N-linked glycosylation and its impact on the electrophoretic mobility and function of the human proton-coupled folate transporter (HsPCFT). *Biochim. Biophys. Acta, Biomembr* 2008, 1778 (6), 1407–1414.
- (32). Wang Y; Zhao R; Goldman ID Characterization of a folate transporter in HeLa cells with a low pH optimum and high affinity for pemetrexed distinct from the reduced folate carrier. *Clin. Cancer Res* 2004, 10 (18), 6256–6264. [PubMed: 15448015]
- (33). Lehtinen MK; Walsh CA Neurogenesis at the brain-cerebrospinal fluid interface. *Annu. Rev. Cell Dev. Biol* 2011, 27, 653–679. [PubMed: 21801012]
- (34). Lehtinen M; Zappaterra M; Chen X; Yang Y; Hill A; Lun M; Maynard T; Gonzalez D; Kim S; Ye P; et al. The cerebrospinal fluid provides a proliferative niche for neural progenitor cells. *Neuron* 2011, 69 (5), 893–905. [PubMed: 21382550]
- (35). Bozard BR; Ganapathy PS; Duplantier J; Mysona B; Ha Y; Roon P; Smith R; Goldman ID; Prasad P; Martin PM; et al. Molecular and biochemical characterization of folate transport proteins in retinal müller cells. *Invest. Ophthalmol. Visual Sci* 2010, 51 (6), 3226–3235. [PubMed: 20053979]
- (36). Wani NA; Nada R; Kaur J Biochemical and molecular mechanisms of folate transport in rat pancreas; interference with ethanol ingestion. *PLoS One* 2011, 6 (12), e28599. [PubMed: 22163044]
- (37). Weksler BB Blood-brain barrier-specific properties of a human adult brain endothelial cell line. *FASEB J.* 2005, 19 (13), 1872–1874. [PubMed: 16141364]
- (38). Halwachs S; Lakoma C; Gebhardt R; Schafer I; Seibel P; Honscha W Dioxin mediates downregulation of the reduced folate carrier transport activity via the arylhydrocarbon receptor signalling pathway. *Toxicol. Appl. Pharmacol* 2010, 246 (1–2), 100–106. [PubMed: 20451541]
- (39). Durk MR; Chan GNY; Campos CR; Peart JC; Chow ECY; Lee E; Cannon RE; Bendayan R; Miller DS; Pang KS 1 $\alpha$ ,25-Dihydroxyvitamin D3-liganded vitamin D receptor increases expression and transport activity of P-glycoprotein in isolated rat brain capillaries and human and rat brain microvessel endothelial cells. *J. Neurochem* 2012, 123 (6), 944–953. [PubMed: 23035695]
- (40). Durk MR; Han K; Chow ECY; Ahrens R; Henderson JT; Fraser PE; Pang KS 1 $\alpha$ ,25-Dihydroxyvitamin D3 reduces cerebral amyloid- $\beta$  accumulation and improves cognition in mouse models of Alzheimer's disease. *J. Neurosci* 2014, 34 (21), 7091–7101. [PubMed: 24849345]
- (41). Eloranta JJ; Hiller C; Jüttner M; Kullak-Ublick G a. The SLC01A2 gene, encoding human organic anion-transporting polypeptide 1A2, is transactivated by the vitamin D receptor. *Mol. Pharmacol* 2012, 82 (1), 37–46. [PubMed: 22474172]
- (42). Geller J; Kronn D; Jayabose S; Sandoval C Hereditary folate malabsorption: family report and review of the literature. *Medicine (Philadelphia, PA, U. S.)* 2002, 81 (1), 51–68.
- (43). Torres A; Newton B; Crompton B; Borzutzky A; Neufeld E; Notarangelo L; Berry G CSF 5-Methyltetrahydrofolate serial monitoring to guide treatment of congenital folate malabsorption due to proton-coupled folatetransporter (PCFT) deficiency. *JIMD Rep.* 2015, 24, 91–96. [PubMed: 26006721]
- (44). Perez-Duenas B; Ormazabal A; Toma C; Torrico B; Cormand B; Serrano M; Sierra C; De Grandis E; Marfa MP; Garcia-Cazorla A; et al. Cerebral folate deficiency syndromes in

childhood: clinical, analytical, and etiologic aspects. *Arch. Neurol* 2011, 68 (5), 615–621. [PubMed: 21555636]

- (45). Ormazábal A; Perez-Dueñas B; Sierra C; Urreizti R; Montoya J; Serrano M; Campistol J; García-Cazorla A; Pineda M; Artuch R Folate analysis for the differential diagnosis of profound cerebrospinal fluid folate deficiency. *Clin. Biochem* 2011, 44 (8–9), 719–721. [PubMed: 21396357]
- (46). Chow EC; Sun H; Khan AA; Groothuis GM; Pang KS Effects of 1 $\alpha$ ,25-dihydroxyvitamin D3 on transporters and enzymes of the rat intestine and kidney in vivo. *Biopharm. Drug Dispos* 2009, 31 (1), 91–108.
- (47). Assaraf YG The role of multidrug resistance efflux transporters in antifolate resistance and folate homeostasis. *Drug Resist. Updates* 2006, 9 (4–5), 227–246.
- (48). Chow ECY; Quach HP; Vieth R; Pang KS Temporal changes in tissue 1 $\alpha$ ,25-dihydroxyvitamin D3, vitamin D receptor target genes, and calcium and PTH levels after 1,25(OH)2D3 treatment in mice. *Am. J. Physiol. Endocrinol. Metab* 2013, 304 (10), E977–89. [PubMed: 23482451]

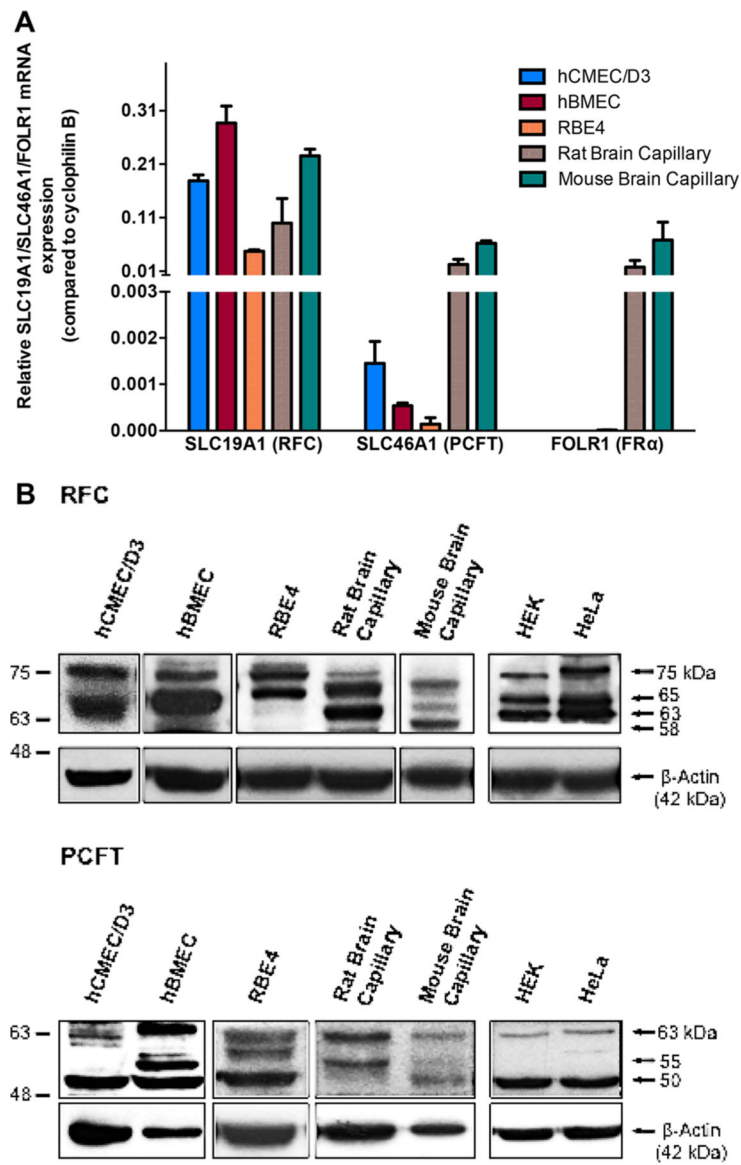


**Figure 1.** Relative expression of major folate transport systems in various *in vitro* and *ex vivo* models of the BBB. (A) mRNA expression of human, rat, or mouse *SLC19A1/Slc19a1* (RFC), *SLC46A1/Slc46a1* (PCFT), and *FOLR1/Folr1* (FR $\alpha$ ) genes were determined in immortalized (hCMEC/D3) and primary (hBMEC) cultures of human brain microvessel endothelial cells, immortalized cultures of rat brain microvessel endothelial cells (RBE4), and rodent brain capillaries using TaqMan gene expression assay. Results are presented as mean relative mRNA expression  $\pm$  SEM normalized to the housekeeping human/rat/mouse cyclophilin B gene from  $n = 3$  independent experiments. (B) Immunoblot analysis of RFC and PCFT protein expression was performed in the same BBB model systems. HEK293 and HeLa cells served as positive controls, while actin was used as a loading control. Multiple protein bands for RFC and PCFT are indicative of differential glycosylation of these

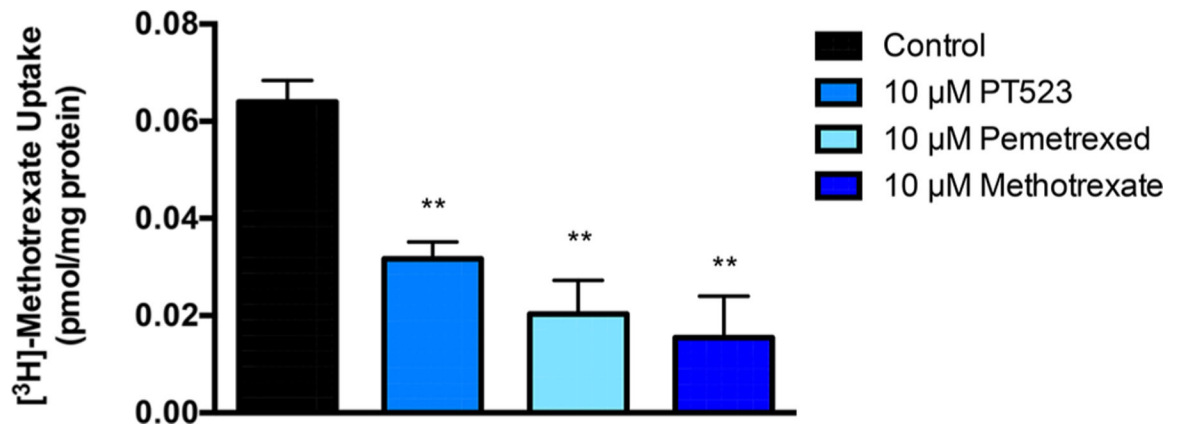
transmembrane proteins. A representative blot is shown from  $n = 3$  independent experiments.

Author Manuscript

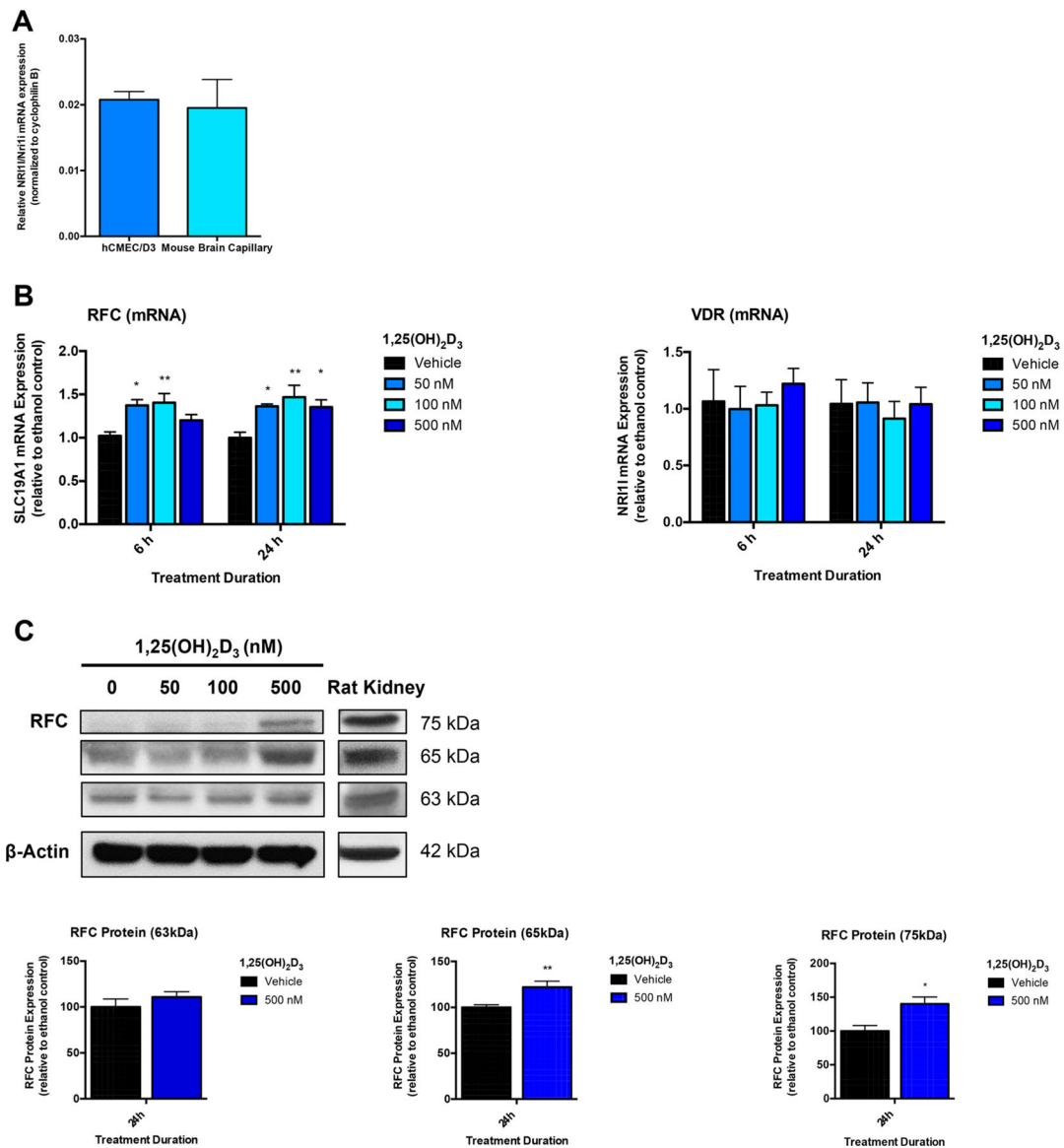
Author Manuscript

Author Manuscript

Author Manuscript



**Figure 2.** Methotrexate uptake by hCMEC/D3 cells. The inhibitory effects of PT523 (10  $\mu$ M) or pemetrexed (10  $\mu$ M), high-affinity substrates for RFC, or excess unlabeled methotrexate (10  $\mu$ M) on [<sup>3</sup>H]-methotrexate uptake (50 nM) was measured over 5 s at pH 7.4 and 37 °C. Results are presented as mean  $\pm$  SEM of  $n = 3-4$  independent experiments. \*\*,  $p < 0.01$ .

**Figure 3.**

Effect of calcitriol treatment on RFC expression in hCMEC/D3 cells. (A) mRNA expression of human *NRII*/rodent *NriI* gene was determined in immortalized cultures of human brain microvessel endothelial (hCMEC/D3) cells and isolated mouse brain capillaries using TaqMan gene expression assay. Results are presented as mean relative mRNA expression  $\pm$  SEM normalized to the housekeeping human cyclophilin B gene from  $n = 3$  independent experiments. Significant increases in *SLC19A1* mRNA (B) and RFC protein (C) expression were observed in hCMEC/D3 cells treated with calcitriol (50–500 nM) for 6 or 24 h compared to vehicle (ethanol) control. Multiple protein bands for RFC (63–75 kDa) are indicative of differential glycosylation of the transmembrane protein. Rat kidney lysates served as positive control, while actin was used as a loading control. Results are presented as mean  $\pm$  SEM for  $n = 3$ –4 independent experiments. \*,  $p < 0.05$ ; \*\*,  $p < 0.01$ .



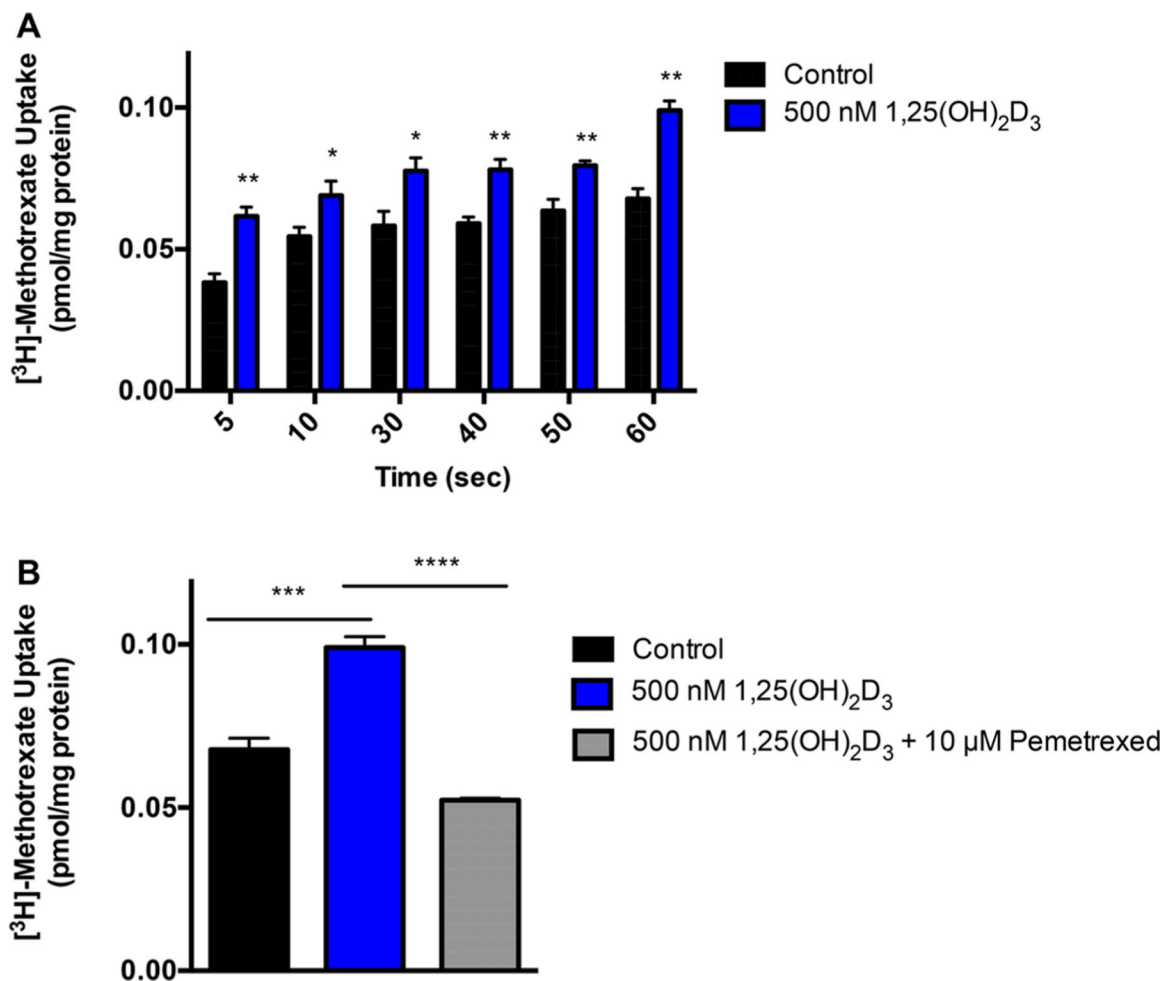


**Figure 4.** Effect of calcitriol (500 nM) or ethanol (vehicle control) treatment for 24 h on methotrexate uptake. (A) Cellular uptake of [<sup>3</sup>H]-methotrexate (50 nM) was measured over 1 min at pH 7.4 and 37 °C. (B) Uptake of [<sup>3</sup>H]-methotrexate (50 nM) by calcitriol-treated hCMEC/D3 cells, measured after 1 min, was inhibited by pemetrexed (10 μM). Results are presented as mean ± SEM for *n* = 4 independent experiments. \*, *p* < 0.05; \*\*, *p* < 0.01; \*\*\*, *p* < 0.001; \*\*\*\*, *p* < 0.0001.

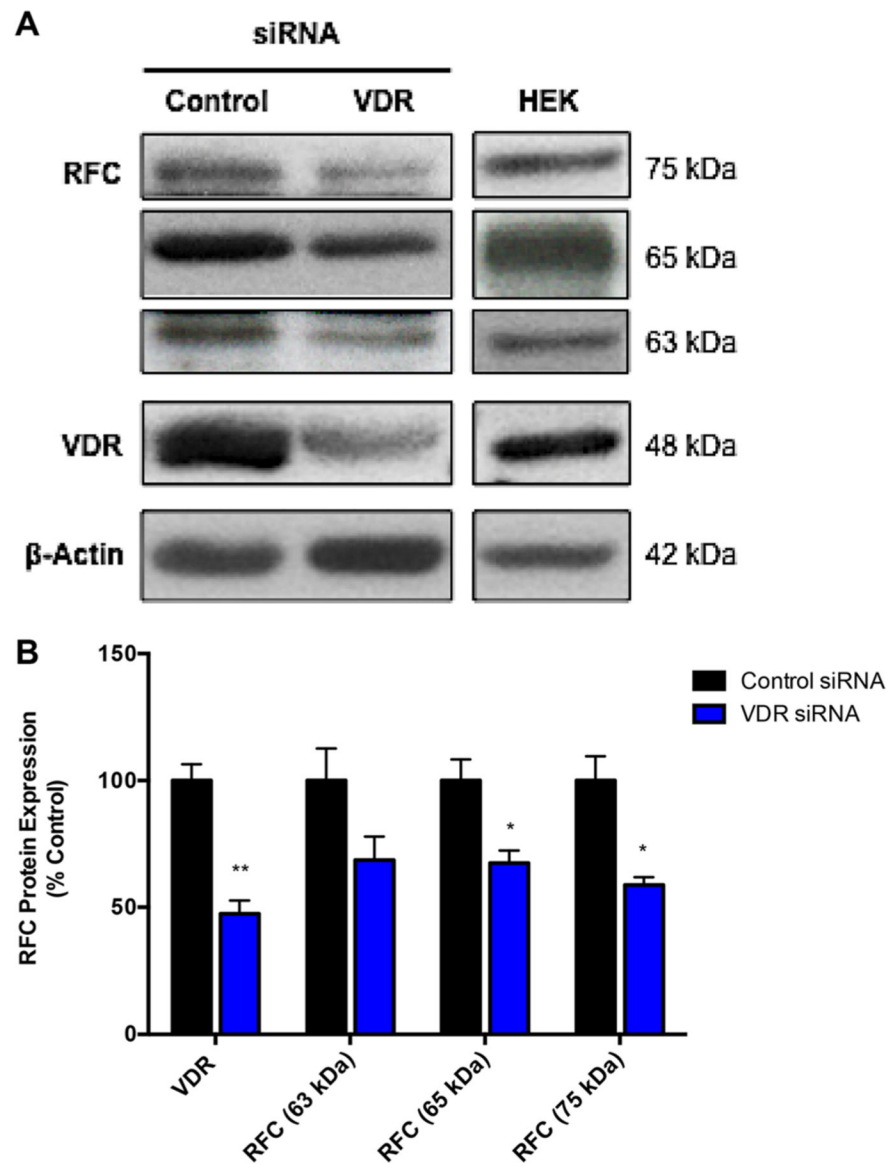


**Figure 5.** Effect of VDR down-regulation on RFC expression in hCMEC/D3 cells. (A) Significant decreases in VDR and RFC protein expression were observed in cells transfected with VDR siRNA compared to scrambled siRNA-treated control. Multiple protein bands for RFC (63–75 kDa) are indicative of differential glycosylation of the transmembrane protein. The HEK293 cell line served as positive control, while actin was used as a loading control. (B) Relative levels of VDR and RFC expression were determined by densitometric analyses. Results are expressed as percentage change normalized to control siRNA and reported as mean  $\pm$  SEM for  $n = 3$  independent experiments. \*,  $p < 0.05$ ; \*\*,  $p < 0.01$ .

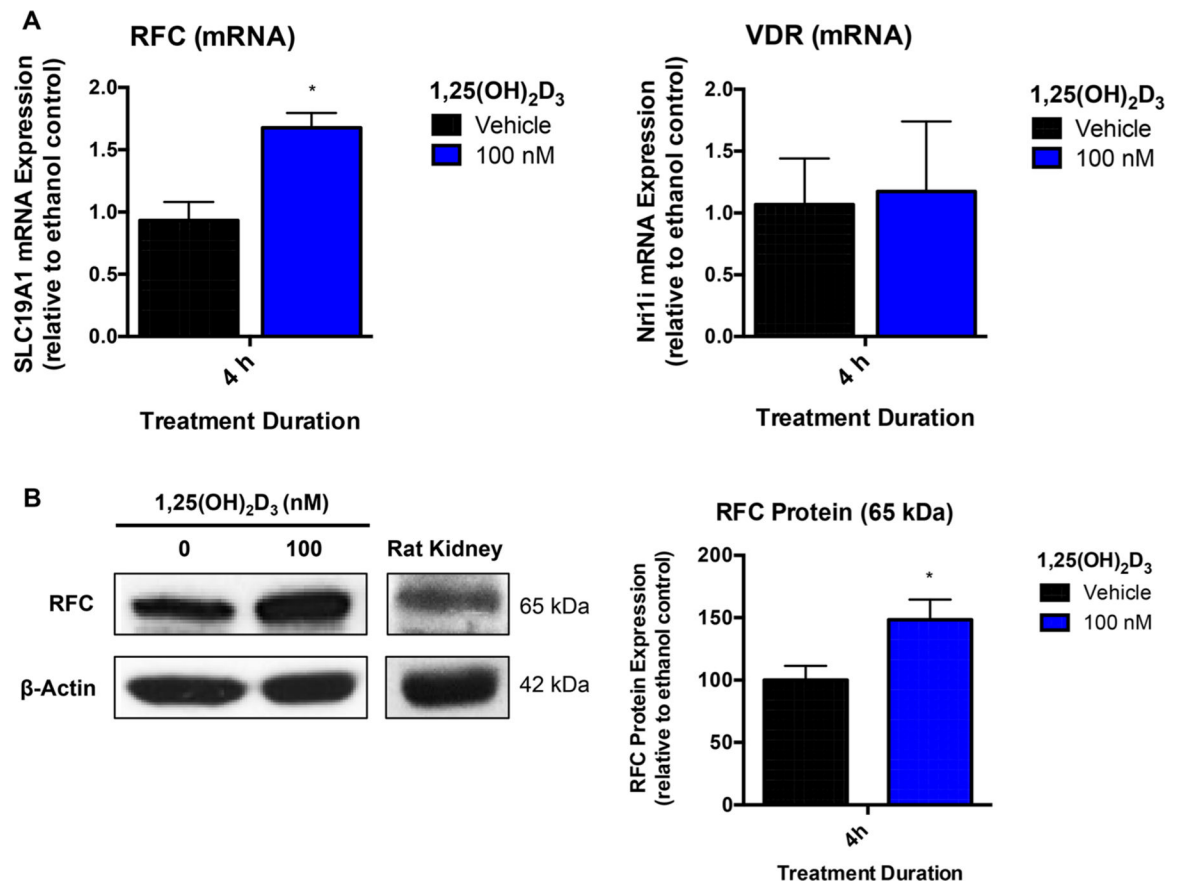


**Figure 6.** Effect of calcitriol treatment on RFC expression in isolated mouse brain capillaries. Significant increases in *SLC19A1* mRNA (A) and RFC protein (B) expression were observed in mouse brain capillaries treated with 100 nM calcitriol for 4 h compared to vehicle (ethanol) control. Results are presented as mean  $\pm$  SEM for  $n = 3$  independent experiments, where each experiment contained pooled brain tissues from 3 to 4 animals per group. \*,  $p < 0.05$ .